

MIMO Precoding in Underlay Cognitive Radio Systems with Completely Unknown Primary CSI

Amitav Mukherjee, Minyan Pei, and A. Lee Swindlehurst, *Fellow, IEEE*

Abstract—This paper studies a novel underlay MIMO cognitive radio (CR) system, where the instantaneous or statistical channel state information (CSI) of the interfering channels to the primary receivers (PRs) is completely unknown to the CR. For the single underlay receiver scenario, we assume a minimum information rate must be guaranteed on the CR main channel whose CSI is known at the CR transmitter. We first show that low-rank CR interference is preferable for improving the throughput of the PRs compared with spreading less power over more transmit dimensions. Based on this observation, we then propose a rank minimization CR transmission strategy assuming a minimum information rate must be guaranteed on the CR main channel. We propose a simple solution referred to as frugal waterfilling (FWF) that uses the least amount of power required to achieve the rate constraint with a minimum-rank transmit covariance matrix. We also present two heuristic approaches that have been used in prior work to transform rank minimization problems into convex optimization problems. The proposed schemes are then generalized to an underlay MIMO CR downlink network with multiple receivers. Finally, a theoretical analysis of the interference temperature and leakage rate outage probabilities at the PR is presented for Rayleigh fading channels. We demonstrate that the direct FWF solution leads to higher PR throughput even though it has higher interference “temperature (IT) compared with the heuristic methods and classic waterfilling, which calls into question the use of IT as a metric for CR interference.

Index Terms—MIMO cognitive radio, spectrum underlay, outage probability, interference mitigation.

I. INTRODUCTION

Cognitive radios (CRs) have gained prominence as an efficient method of improving spectrum utilization by allowing coexistence with licensed networks, which is denoted as dynamic spectrum access (DSA). One popular variant of DSA is known as spectrum underlay, where underlay cognitive transmitters (UCTs) operate simultaneously with licensed (primary) users, but adapt their transmission parameters so as to confine the interference perceived at the primary receivers (PRs) to a pre-specified threshold [1]. Therefore, a fundamental challenge for the CR is to balance between maximizing its own transmit rate and minimizing the interference it causes to the PRs. In CR networks with single-antenna nodes, this is usually achieved by exploiting some knowledge of the interfering cross-channels to the PRs at the UCT and performing some admission control algorithms with power control [2].

If UCTs are equipped with multiple antennas, the available spatial degrees of freedom can be used to mitigate interference

to the PRs during transmission to the underlay receivers. Multi-antenna CR networks have recently received extensive attention, assuming some knowledge of the interfering cross-channels to the PRs at the UCT, either perfect PR cross-channel state information (CSI) [3]-[5], perturbed PR CSI [6]-[8], or statistical PR CSI [9]-[12]. However, the UCT may not have the luxury of knowing the CSI of the cross links to the PRs, as the primary system would not deliberately coordinate the collection of CSI for the CR system.

In this work, we consider the novel scenario where both the realizations and distribution of the PR cross-channels are *completely unknown* at the CR, thereby precluding the overwhelming majority of existing spectrum underlay schemes in the literature [3], [4]. Such a scenario of completely-unknown PR CSI is relevant in a number of instances, for example, when the PR transmits intermittently and therefore stymies attempts to learn the cross-channel, when channels are varying rapidly over time, when the PT and PR do not employ time-division duplexing as assumed in [10], [11] among others, or when there are a plurality of active PTs/UCTs and it is impossible to indirectly estimate specific channels.

Specifically, we propose a rank minimization transmission strategy for the UCT while maintaining a minimum information rate on the CR link, and we present a simple solution referred to as frugal waterfilling (FWF) that uses the least amount of power required to achieve the rate constraint with a minimum-rank covariance matrix. In the context of MIMO interference channels (for which the CR underlay network is a special case), rank-minimization has been shown to be a reinterpretation of interference alignment [14], but this approach requires knowledge of interfering cross-channels and treats the overall system sum rate or degrees-of-freedom as the performance metric, assumptions which are both markedly different from the underlay CR scenario we consider.

We also describe two heuristic approaches that have been used in prior work to transform rank minimization problems (RMP) into problems that can be solved via convex optimization. These approaches approximate the rank objective function with two relaxations, one based on the nuclear norm [22], and the other on a log-determinant function [23]. We show theoretically and via numerical simulation that minimizing the rank of the UCT spatial covariance matrix leads to the highest PR throughput in general Rayleigh-fading channels, compared with spreading the transmit power over more dimensions. Furthermore, our simulations indicate that FWF provides a higher PR throughput than the nuclear-norm and log-det heuristic solutions, even though FWF has a higher interference “temperature” (IT). This suggests that the commonly used

The authors are with the Dept. of EECS, University of California, Irvine, CA 92697-2625, USA. (e-mail: {amukherj; mpei; swindle}@uci.edu)

This work was supported by the U.S. ARO under MURI grant W911NF-07-1-0318, and by the NSF under grant CCF-1117983.

IT metric does not accurately capture the impact of the CR interference on PR performance. Instead, we propose a metric based on interference leakage (IL) rate that more accurately reflects the influence of the CR interference.

This paper is organized as follows. The underlay system model is introduced in Section II. PR CSI-unaware UCT transmit strategies for a single UCR are presented in Section III. The generalization to the underlay downlink with multiple UCRs is shown in Section V. A random matrix-theoretic analysis of the primary outage probability due to the proposed strategies is given in Section VI. The penultimate Section VII presents numerical simulations for various underlay scenarios, and we conclude in Section VIII.

Notation: We will use $\mathcal{CN}(\mathbf{0}, \mathbf{Z})$ to denote a circularly symmetric complex Gaussian distribution with zero mean and covariance matrix \mathbf{Z} , $\mathcal{E}\{\cdot\}$ to denote expectation, $\text{vec}(\cdot)$ the matrix column stacking operator, $(\cdot)^T$ the transpose, $(\cdot)^H$ the Hermitian transpose, $(\cdot)^{-1}$ the matrix inverse, $\text{Tr}(\cdot)$ the trace operator, $|\cdot|$ or \det the matrix determinant, $\text{diag}(\mathbf{a})$ a diagonal matrix with the elements of \mathbf{a} on the main diagonal, $|\mathbf{A}|_{i,j}$ the (i, j) element of \mathbf{A} , $\Gamma(x)$ the gamma function, and \mathbf{I} is the identity matrix.

II. SYSTEM MODEL

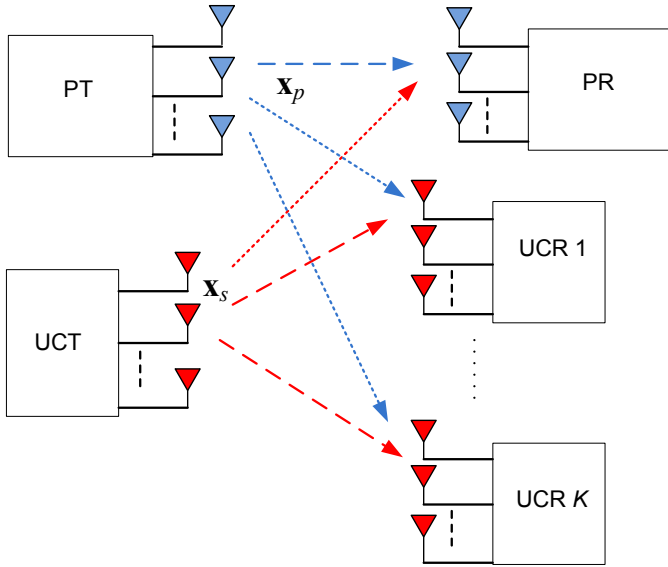


Fig. 1. Cognitive radio network with a multi-antenna underlay CR transmitter, K underlay receivers, and a single MIMO PT-PR pair.

A generic MIMO underlay CR network with K multi-antenna underlay receivers is shown in Fig. 1, where a primary system and an underlay CR system share the same spectral band. Since the UCT transmit strategies are independent of the cross-channels to primary users, the numbers of PRs and PTs and their array sizes can be made arbitrary; however to simplify notation we will consider a solitary multi-antenna PT-PR pair. To introduce the problem we first consider the scenario with a single UCR, and generalize to the case of $K > 1$ in Sec. V.

We consider a multi-antenna UCT equipped with N_a antennas, which transmits a signal vector $\mathbf{x}_s \in \mathbb{C}^{N_a \times 1}$, to its

N_s -antenna underlay cognitive receiver (UCR). The PT is equipped with N_p antennas and transmits signal $\mathbf{x}_p \in \mathbb{C}^{N_p \times 1}$ to the N_r -antenna PR. Thus, the UCR observes

$$\mathbf{y}_s = \mathbf{G}_1 \mathbf{x}_s + \mathbf{G}_2 \mathbf{x}_p + \mathbf{n}_s, \quad (1)$$

where $\mathbf{G}_1 \in \mathbb{C}^{N_s \times N_a}$, $\mathbf{G}_2 \in \mathbb{C}^{N_s \times N_p}$ are the complex MIMO channels from the UCT and PT, and $\mathbf{n}_s \sim \mathcal{CN}(\mathbf{0}, \sigma_s^2 \mathbf{I})$ is complex additive white Gaussian noise. We assume Gaussian signaling with zero mean and second-order statistics $\mathcal{E}\{\mathbf{x}_s \mathbf{x}_s^H\} = \mathbf{Q}_s$, and the average UCT transmit power is assumed to be bounded:

$$\text{Tr}(\mathbf{Q}_s) \leq P_s.$$

The signal at the PR is given by

$$\mathbf{y}_p = \mathbf{H}_1 \mathbf{x}_p + \mathbf{H}_2 \mathbf{x}_s + \mathbf{n}_p, \quad (2)$$

where $\mathbf{H}_1 \in \mathbb{C}^{N_p \times N_r}$, $\mathbf{H}_2 \in \mathbb{C}^{N_r \times N_a}$ are the channels from the PU and CR transmitters (assumed to be full-rank), and $\mathbf{n}_p \sim \mathcal{CN}(\mathbf{0}, \sigma_p^2 \mathbf{I})$ is complex additive white Gaussian noise. The primary signal is also modeled as a zero-mean complex Gaussian signal with covariance matrix \mathbf{Q}_p and average power constraint $\text{Tr}(\mathbf{Q}_p) \leq P_p$. We will assume \mathbf{Q}_p is fixed and the channels are mutually independent and each composed of i.i.d. zero-mean circularly symmetric complex Gaussian entries, and focus our attention on the design of the UCT transmit signal.

We assume there is no cooperation between the PT and UCT during transmission, and that both receivers treat interfering signals as noise. The network is essentially an asymmetric 2-user MIMO interference channel, where the UCT attempts to minimize the interference to the PR, but no such reciprocal gesture is made by the PT. The interference covariance matrix at the PR is

$$\mathbf{K}_p = \mathbf{H}_2 \mathbf{Q}_s \mathbf{H}_2^H. \quad (3)$$

Define the interference temperature at the PR as [3]-[12]

$$T_p(\mathbf{Q}_s) = \text{Tr}(\mathbf{K}_p). \quad (4)$$

Without knowledge of \mathbf{H}_2 or its distribution, the UCT cannot directly optimize the PR interference temperature or outage probability as in existing underlay proposals [3]-[12]. To our best knowledge, precoding strategies and performance analyses for MIMO underlay systems with completely unknown primary CSI have not been presented in the literature thus far. In addition to [3]-[13] not being applicable, the blind interference alignment method for the 2-user MIMO interference channel [15] is also precluded since it requires knowledge of the cross-channel coherence intervals, which we assume is also unknown. In [13], a blind underlay precoding scheme is proposed where the MIMO CR iteratively updates its spatial covariance by observing the transmit power of a solitary PT. The UCT attempts to infer the least-harmful spatial orientation towards the PR, but requires that the PT employ a power control scheme monotonic in the interference caused by the CR, and that the cross-channel remains constant during the learning process. In contrast, we investigate simple non-iterative CR precoding strategies which do not impose any restrictions on the PT transmission strategy or number of PTs, or cross-channel coherence intervals.

The PT achieves the following rate on its link:

$$R_p(\mathbf{Q}_s) = \log_2 \left| \mathbf{I} + \mathbf{H}_1 \mathbf{Q}_p \mathbf{H}_1^H (\mathbf{K}_p + \sigma_p^2 \mathbf{I})^{-1} \right|. \quad (5)$$

Similarly, the achievable rate on the CR link is

$$R_s(\mathbf{Q}_s) = \log_2 \left| \mathbf{I} + \mathbf{G}_1 \mathbf{Q}_s \mathbf{G}_1^H (\mathbf{K}_s + \sigma_s^2 \mathbf{I})^{-1} \right| \quad (6)$$

where $\mathbf{K}_s = \mathbf{G}_2 \mathbf{Q}_p \mathbf{G}_2^H$ represents the interference from the PT.

III. A RANK MINIMIZATION STRATEGY FOR CSI-UNAWARE UNDERLAY TRANSMISSION

We now expound on the fundamental motivation underlying the UCT transmission strategies proposed in this work. As we have seen, due to a lack of knowledge of \mathbf{H}_2 or its distribution, the UCT cannot directly optimize the PU interference temperature. Hence, we propose an alternative transmission strategy where the UCT tries to minimize a measure of the interference caused to the PR in a “best-effort” sense, while achieving a target data rate to the UCR. Assuming that \mathbf{Q}_p is fixed, we first show that in the clairvoyant case where the UCT has some knowledge of the channel to the PR (\mathbf{H}_2), a rank-1 UCT covariance matrix \mathbf{Q}_s causes least interference to the primary link, which is described in the following proposition.

Proposition 1: The optimal solution to the clairvoyant problem

$$\max_{\mathbf{Q}_s} \mathcal{E} \{R_p(\mathbf{Q}_s)\} \quad (7a)$$

$$\text{s.t. } R_s(\mathbf{Q}_s) = R_b \quad (7b)$$

$$\text{Tr}(\mathbf{Q}_s) \leq P_s \quad (7c)$$

$$\mathbf{Q}_s \succeq \mathbf{0}. \quad (7d)$$

that maximizes the average PR rate is of rank one, i.e., $\text{rank}(\mathbf{Q}_s^*) = 1$.

Proof: Since $\mathbf{Q}_s \succeq \mathbf{0}$, it can be expressed as $\mathbf{Q}_s = \mathbf{U} \mathbf{\Lambda} \mathbf{U}^H$, where $\mathbf{\Lambda}$ is the diagonal matrix of eigenvalues of \mathbf{Q}_s and \mathbf{U} is the unitary matrix with columns consisting of the eigenvectors of \mathbf{Q}_s . Defining $\tilde{\mathbf{H}}_2 = \mathbf{H}_2 \mathbf{U}$, it follows from Lemma 5 in [16] that the distribution of $\tilde{\mathbf{H}}_2$ is the same as that of \mathbf{H}_2 . As a result, the average PU rate can be expressed as

$$\begin{aligned} R_p(\mathbf{Q}_s) &= \Phi(\mathbf{\Lambda}) \\ &= \mathcal{E} \left\{ \log_2 \left[\det \left(\mathbf{I} + \mathbf{H}_1 \mathbf{Q}_p \mathbf{H}_1^H \left(\tilde{\mathbf{H}}_2 \mathbf{\Lambda} \tilde{\mathbf{H}}_2^H + \sigma_p^2 \mathbf{I} \right)^{-1} \right) \right] \right\} \end{aligned}$$

Thus, the problem we considered is essentially equivalent to constructing the diagonal matrix $\mathbf{\Lambda}$ with real nonnegative entries so as to maximize $\Phi(\mathbf{\Lambda})$ under the constraint $\text{Tr}(\mathbf{\Lambda}) = P_s$.

From [25, Lemma 3],[26], we have that $\Phi(\mathbf{\Lambda})$ is a convex function of $\mathbf{\Lambda}$. Note that given any permutation matrix $\mathbf{\Pi}$, we see (using Lemma 5 in [16] again) that

$$\Phi(\mathbf{\Pi} \mathbf{\Lambda} \mathbf{\Pi}^H) = \Phi(\mathbf{\Lambda}).$$

From convexity, we have

$$\Phi \left(\frac{1}{N_a!} \sum_{\mathbf{\Pi}} \mathbf{\Pi} \mathbf{\Lambda} \mathbf{\Pi}^H \right) \leq \frac{1}{N_a!} \sum_{\mathbf{\Pi}} \Phi(\mathbf{\Pi} \mathbf{\Lambda} \mathbf{\Pi}^H) = \Phi(\mathbf{\Lambda})$$

where we have used Jensen’s inequality. From the transmit power constraint, we have $\frac{1}{N_a!} \sum_{\mathbf{\Pi}} \mathbf{\Pi} \mathbf{\Lambda} \mathbf{\Pi}^H = (P_s/N_a) \mathbf{I}_{N_a}$. Thus, we have proved that the least PU rate is obtained by $\mathbf{\Lambda} = (P_s/N_a) \mathbf{I}_{N_a}$. Further, due to convexity, we can argue that the largest PU rate is obtained by a point farthest away from $\mathbf{\Lambda} = (P_s/N_a) \mathbf{I}_{N_a}$. Thus, we want $\mathbf{\Lambda}^* = \text{diag}(\lambda_1^*, \dots, \lambda_{N_a}^*)$ that satisfy [21]

$$\max \sum_{i=1}^{N_a} \left(\lambda_i - \frac{P_s}{N_a} \right)^2 \quad \text{s.t. } \sum_{i=1}^{N_a} \lambda_i = P_s$$

Now,

$$\begin{aligned} \sum_{i=1}^{N_a} \left(\lambda_i - \frac{P_s}{N_a} \right)^2 &= \sum_{i=1}^{N_a} \lambda_i^2 - 2 \frac{P_s}{N_a} \sum_{i=1}^{N_a} \lambda_i + \frac{P_s^2}{N_a} \\ &= P_s^2 \left(\sum_{i=1}^{N_a} \left(\frac{\lambda_i}{P_s} \right)^2 - \frac{1}{N_a} \right) \\ &\leq P_s^2 \left(\sum_{i=1}^{N_a} \frac{\lambda_i}{P_s} - \frac{1}{N_a} \right) \\ &= P_s^2 \left(1 - \frac{1}{N_a} \right) \end{aligned}$$

where we used $\sum_{i=1}^{N_a} \left(\frac{\lambda_i}{P_s} \right)^2 \leq \sum_{i=1}^{N_a} \frac{\lambda_i}{P_s} = 1$, and the equality is satisfied by any $(\lambda_1^*, \dots, \lambda_{N_a}^*)$ with all zeros except for one nonzero entry. Hence, we conclude that $\text{rank}(\mathbf{Q}_s^*) = \text{rank}(\mathbf{\Lambda}^*) = 1$. ■

Therefore, in the clairvoyant case where the UCT has some knowledge of the primary CSI, a rank-1 \mathbf{Q}_s causes least interference to the primary link and full-rank \mathbf{Q}_s causes most interference¹. Of course, the optimal \mathbf{Q}_s will depend on the PR CSI, which we have assumed is unavailable. Still, the result motivates the use of a low-rank transmit covariance at the UCT. It is evident that the UCT does not actually require knowledge of the PR CSI to minimize the rank of \mathbf{Q}_s needed to achieve a rate target R_b on the CR link. To exploit this observation, we henceforth pose the UCT precoder design problem when the PR CSI is completely unknown as

$$(P0) : \quad \min \quad \text{rank}(\mathbf{Q}_s) \quad (8a)$$

$$\text{s.t. } R_s(\mathbf{Q}_s) = R_b \quad (8b)$$

$$\text{Tr}(\mathbf{Q}_s) \leq P_s \quad (8c)$$

$$\mathbf{Q}_s \succeq \mathbf{0}. \quad (8d)$$

This is a rank-minimization problem (RMP), and in general is computationally hard to solve since the rank function is quasi-concave and not convex. As explained below, however, in this case a simple waterfilling solution can be obtained. In [24], the mutual information of the CR link is maximized subject to an interference temperature constraint and arbitrary transmit covariance rank constraints, which implies knowledge of PR CSI and thus differs from this work.

¹This notion has been echoed in prior art on MIMO interference channels [17], [18]

IV. SOLUTIONS FOR THE RANK MINIMIZATION DESIGN

Notice that the design problem (P0) is ill-posed in the sense that there are potentially an infinite number of solutions. Suppose that we find one minimum-rank solution to (P0) such that $\mathbf{Q}_s = \mathbf{U}\mathbf{\Lambda}\mathbf{U}^H$ for some unitary matrix \mathbf{U} and diagonal matrix $\mathbf{\Lambda}$ satisfies $R_s(\mathbf{Q}_s) = R_b$, $\text{Tr}(\mathbf{\Lambda}) \leq P_s$. If the required power $\text{Tr}(\mathbf{\Lambda})$ is strictly smaller than P_s , then we could find an infinite number of solutions by making small perturbations to \mathbf{U} , which while leading to a higher power requirement, still would require less power than P_s . Obviously, the solution with least power is more desirable for our underlay CR system in order to minimize the interference caused to the PR, and this solution can easily be found using the *Frugal Waterfilling* (FWF) approach described next.

A. FWF Approach

The FWF solution seeks to find the least amount of power required to achieve the CR rate target of R_b with the minimum rank transmit covariance \mathbf{Q}_s . The optimization problem can be solved using a combination of the classic waterfilling (CWF) algorithm and a simple bisection line search. The description for FWF is outlined as Algorithm IV-A.1 below. In brief, FWF cycles through the possible number of transmit dimensions in ascending order starting with a rank-one \mathbf{Q}_s , and at each step computes the transmit power required to meet the rate constraint R_b based on CWF. This requires a simple line search over the transmit power for each step. Once a solution is found that satisfies the transmit power constraint, the algorithm terminates. If no feasible solution is found for all N_a transmit dimensions, the CR link will be in outage.

Algorithm IV-A.1 Frugal Waterfilling for UCT Rank/Power Tradeoff [19]

Require: $P_s > 0, R_b > 0$

set $r = \text{rank}(\mathbf{G}_1)$

for $M = 1$ to r **do**

Solve:

$$p(M) = \min \text{Tr}(\mathbf{Q}_s)$$

$$\text{s. t. } \log_2 \left| \mathbf{I} + \mathbf{G}_1 \mathbf{Q}_s \mathbf{G}_1^H (\mathbf{K}_s + \sigma_s^2 \mathbf{I})^{-1} \right| = R_b .$$

end for

if $p(r) > P_s$ **then**

Declare outage

else

CWF solution: $N = \arg \min_M p(M)$;

FWF solution: $N = \arg \min_M$;

\mathbf{Q}_s determined by waterfilling $p(N)$ over N largest singular values of $(\mathbf{K}_s + \sigma_s^2 \mathbf{I})^{-1/2} \mathbf{G}_1$

end if

The FWF algorithm was presented in brief without analysis by the authors in [19], and through simulation were shown to be an effective transmission strategy in conventional downlink, wiretap, and underlay networks. While FWF finds an efficient solution to (P0), in general rank minimization problems are

difficult to solve and often require exponential-time complexity. Consequently, heuristic approximations to the matrix rank have been proposed as alternatives in order to yield simpler optimization problems. In particular, the nuclear norm [22] and log-determinant [23] heuristics have been proposed in order to convexify RMP problems like (P0) and provide approximate solutions with polynomial-time complexity. In the discussion below, we show how these approximations can be applied to the RMP we consider in this paper.

B. Nuclear Norm and Log-det Heuristic

The *nuclear norm heuristic* is based on the fact the nuclear norm (sum of the singular values of a matrix) is the convex envelope of the rank function on the unit ball. When the matrix is positive semidefinite, the nuclear norm is the same as the trace function. As a result, the design problem (P0) can be formulated as follows:

$$\begin{aligned} \text{(P1)} : \quad & \min \quad \text{Tr}(\mathbf{Q}_s) \\ & \text{s.t.} \quad R_s(\mathbf{Q}_s) = R_b \\ & \quad \quad \text{Tr}(\mathbf{Q}_s) \leq P_s \\ & \quad \quad \mathbf{Q}_s \succeq \mathbf{0} . \end{aligned} \quad (9)$$

The nuclear norm heuristic (P1) is a convex optimization problem and can be solved using the CWF algorithm together with a bisection line search (similar to FWF). It is well known that under the CWF algorithm, the lowest transmit power is achieved when $\text{rank}(\mathbf{Q}_s)$ is chosen as large as possible (up to $\text{rank}(\mathbf{G}_1)$). This is clearly contrary to the rank-minimization design formulation, which indicates that the nuclear norm approach for this problem is a poor approximation.

Using the function $\log \det(\mathbf{Q}_s + \delta \mathbf{I})$ as a smooth surrogate for $\text{rank}(\mathbf{Q}_s)$, the *log-det heuristic* can be described as follows:

$$\begin{aligned} \text{(P2)} : \quad & \min \quad \log \det(\mathbf{Q}_s + \delta \mathbf{I}) \\ & \text{s.t.} \quad R_s(\mathbf{Q}_s) = R_b \\ & \quad \quad \text{Tr}(\mathbf{Q}_s) \leq P_s \\ & \quad \quad \mathbf{Q}_s \succeq \mathbf{0} , \end{aligned} \quad (10)$$

where $\delta \geq 0$ can be interpreted as a small regularization constant (we choose $\delta = 10^{-6}$ for numerical examples). Since the surrogate function $\log \det(\mathbf{Q}_s + \delta \mathbf{I})$ is smooth on the positive definite cone, it can be minimized using a local minimization method. We use iterative linearization to find a local minimum to the optimization problem (P2) [23]. Let $\mathbf{Q}_s^{(k)}$ denote the k th iteration of the optimization variable \mathbf{Q}_s . The first-order Taylor series expansion of $\log \det(\mathbf{Q}_s + \delta \mathbf{I})$ about $\mathbf{Q}_s^{(k)}$ is given by

$$\begin{aligned} \log \det(\mathbf{Q}_s + \delta \mathbf{I}) \approx & \log \det(\mathbf{Q}_s^{(k)} + \delta \mathbf{I}) + \\ & \text{Tr}[(\mathbf{Q}_s^{(k)} + \delta \mathbf{I})^{-1}(\mathbf{Q}_s - \mathbf{Q}_s^{(k)})] . \end{aligned} \quad (11)$$

Hence, we could attempt to minimize $\log \det(\mathbf{Q}_s + \delta \mathbf{I})$ by iteratively minimizing the local linearization (11). This leads to

$$\mathbf{Q}_s^{(k+1)} = \text{argmin} \text{Tr}[(\mathbf{Q}_s^{(k)} + \delta \mathbf{I})^{-1} \mathbf{Q}_s] . \quad (12)$$

If we choose $\mathbf{Q}_s^{(0)} = \mathbf{I}$, the first iteration of (12) is equivalent to minimizing the trace of \mathbf{Q}_s . Therefore, this heuristic can

be viewed as a refinement of the nuclear norm heuristic. As a result, we always pick $\mathbf{Q}_s^{(0)} = \mathbf{I}$, so that $\mathbf{Q}_s^{(1)}$ is the result of the trace heuristic, and the iterations that follow try to reduce the rank of $\mathbf{Q}_s^{(1)}$ further.

Note that at each iteration we will solve a weighted trace minimization problem, which is equivalent to the following optimization problem

$$\begin{aligned} \text{(P2-1)} : \quad & \min \quad \text{Tr}(\mathbf{F}^H \mathbf{A} \mathbf{F}) \\ & \text{s.t.} \quad \log_2 \det(\mathbf{I} + \mathbf{F}^H \mathbf{R} \mathbf{F}) = R_b \\ & \quad \text{Tr}(\mathbf{F}^H \mathbf{F}) \leq P_s. \end{aligned} \quad (13)$$

where $\mathbf{A} = (\mathbf{Q}_s^{(k)} + \delta \mathbf{I})^{-1}$, $\mathbf{R} = \mathbf{G}_1^H (\mathbf{G}_2 \mathbf{Q}_p \mathbf{G}_2^H + \sigma_s^2 \mathbf{I})^{-1} \mathbf{G}_1$. This is a Schur-concave optimization problem with multiple trace/log-det constraints. From Theorem 1 in [24], the optimal solution to problem (13) is $\mathbf{F}^* = \mathbf{A}^{-1/2} \mathbf{U} \Sigma$, and $\mathbf{Q}_s^{(k+1)} = \mathbf{F}^* \mathbf{F}^{*H}$ is an optimal solution to (12), where $\mathbf{A}^{-1/2} = \mathbf{U}_A \Lambda_A^{-1/2} \mathbf{U}_A^H$, \mathbf{U}_A and Λ_A are defined in the eigen-decomposition $\mathbf{A} = \mathbf{U}_A \Lambda_A \mathbf{U}_A^H$, \mathbf{U} is a unitary matrix, and $\Sigma = \text{diag}(\sqrt{\mathbf{p}})$ is a rectangular diagonal matrix.

Substituting the optimal solution structure \mathbf{F}^* into (13), we have the following equivalent problem

$$\begin{aligned} \text{(P2-2)} : \quad & \min \quad \text{Tr}(\Sigma \Sigma^H) \\ & \text{s.t.} \quad \log_2 \det(\mathbf{I} + \Sigma^H \mathbf{U}^H \tilde{\mathbf{R}} \mathbf{U} \Sigma) = R_b \\ & \quad \text{Tr}(\mathbf{U}^H \mathbf{A}^{-1} \mathbf{U} \Sigma \Sigma^H) \leq P_s \end{aligned} \quad (14)$$

where $\tilde{\mathbf{R}} = \mathbf{A}^{-1/2} \mathbf{R} \mathbf{A}^{-1/2}$. It is found that the equivalent problem (14) is essentially equivalent to the converse formulation

$$\begin{aligned} \text{(P2-3)} : \quad & \max \quad \log_2 \det(\mathbf{I} + \Sigma^H \mathbf{U}^H \tilde{\mathbf{R}} \mathbf{U} \Sigma) \\ & \text{s.t.} \quad \text{Tr}(\Sigma \Sigma^H) = P_0 \\ & \quad \text{Tr}(\mathbf{U}^H \mathbf{A}^{-1} \mathbf{U} \Sigma \Sigma^H) \leq P_s. \end{aligned} \quad (15)$$

This is because both formulations (14) and (15) describe the same tradeoff curve of performance versus power. Therefore, the quality-constrained problem (P2-2) can be numerically solved by iteratively solving the power-constrained problem (P2-3), combined with the bisection method.

The problem formulation in (P2-3) is a Schur-convex optimization problem with two trace constraints. Using Theorem 1 in [24] again, if we let $\tilde{\mathbf{R}} = \mathbf{U}_{\tilde{\mathbf{R}}} \Lambda_{\tilde{\mathbf{R}}} \mathbf{U}_{\tilde{\mathbf{R}}}^H$ denote the eigen-decomposition of $\tilde{\mathbf{R}}$, then the optimal unitary matrix \mathbf{U} will be chosen as $\mathbf{U}_{\tilde{\mathbf{R}}}$. Denoting $\mathbf{a} = \text{diag}(\mathbf{U}^H \mathbf{A}^{-1} \mathbf{U})$ and letting $\lambda_{\tilde{\mathbf{R}},1} \geq \lambda_{\tilde{\mathbf{R}},2} \geq \dots \geq \lambda_{\tilde{\mathbf{R}},N_a}$ represent the diagonal elements of $\Lambda_{\tilde{\mathbf{R}}}$, the optimal power allocation can be shown to have the form of a *multilevel* waterfilling solution:

$$p_i = \left(\frac{1}{\mu + a_i \nu} - \frac{1}{\lambda_i} \right)^+, \quad i = 1, \dots, N_a \quad (16)$$

where a_i is the i th element of \mathbf{a} , and μ, ν can be shown to be the nonnegative Lagrange multipliers associated with the two power constraints. The algorithmic description for the log-det heuristic approach is outlined in Algorithm IV-B.1.

Algorithm IV-B.1 Iterative log-det heuristic Algorithm for rank-minimization problem

Require: $P_s > 0, R_b > 0,$

set $\delta = 10^{-6}, \Delta = 10^{-3}, k = 0,$

$\mathbf{Q}_s^{(0)} = \mathbf{I}, \mathbf{R} = \mathbf{G}_1^H (\mathbf{K}_s + \sigma_s^2 \mathbf{I})^{-1} \mathbf{G}_1.$

repeat

$\mathbf{A} = (\mathbf{Q}_s^{(k)} + \delta \mathbf{I})^{-1}, \tilde{\mathbf{R}} = \mathbf{A}^{-1/2} \mathbf{R} \mathbf{A}^{-1/2},$

$\text{eig}(\tilde{\mathbf{R}}) = \mathbf{U}_{\tilde{\mathbf{R}}} \Lambda_{\tilde{\mathbf{R}}} \mathbf{U}_{\tilde{\mathbf{R}}}^H.$

set $\mathbf{U} = \mathbf{U}_{\tilde{\mathbf{R}}}, \mathbf{a} = \text{diag}(\mathbf{U}^H \mathbf{A}^{-1} \mathbf{U}).$

Solve:

$\min \quad \mathbf{1}^T \mathbf{p}$

s. t. $\log_2 \left(\prod_i (1 + p_i \lambda_{\tilde{\mathbf{R}},i}) \right) = R_b$

$\mathbf{a}^T \mathbf{p} \leq P_s.$

$\Sigma = \text{diag}(\mathbf{p})$

$\mathbf{F} = \mathbf{A}^{-1/2} \mathbf{U} \Sigma$

$\mathbf{Q}_s^{(k+1)} = \mathbf{F} \mathbf{F}^H$

until $\log_2(\det(\mathbf{Q}_s^{(k)} + \delta \mathbf{I})) - \log_2(\det(\mathbf{Q}_s^{(k+1)} + \delta \mathbf{I})) < \Delta$

if $\mathbf{a}^T \mathbf{p} > P_s$ **then**

Declare outage

else

$\rho = \mathbf{a}^T \mathbf{p} / P_s; \quad \mathbf{Q}_s = \mathbf{Q}_s^{(k+1)}$

end if

V. UNDERLAY CR DOWNLINK

In this section we extend the blind underlay precoding paradigm to a MIMO underlay downlink network with K UCRs. We consider a modified block-diagonalization precoding strategy [27] where multiple data streams are transmitted to each UCR. Let each UCR be equipped with N_s antennas for simplicity, although the proposed precoding schemes hold for heterogeneous receiver array sizes as long as the total number of receive antennas does not exceed N_a . The extension to the case where the UCT serves N_a spatial streams regardless of the total number of receive antennas can be made using the coordinated beamforming approach [27], for example. The received signal at UCR k is now

$$\mathbf{y}_k = \mathbf{G}_{k,1} \mathbf{W}_k \mathbf{s}_{u,k} + \sum_{j \neq k}^{K_u} \mathbf{G}_{k,1} \mathbf{W}_j \mathbf{s}_{u,j} + \mathbf{G}_{k,2} \mathbf{s}_p + \mathbf{n}_k \quad (17)$$

where $\mathbf{G}_{k,1} \in \mathbb{C}^{N_s \times N_a}$ is the main channel, $\mathbf{W}_k \in \mathbb{C}^{N_a \times l_k}$ is the precoding matrix applied to signal $\mathbf{s}_{u,k} \in \mathbb{C}^{l_k \times 1}$ for user k , \mathbf{s}_p is the PT signal received over interfering channel $\mathbf{G}_{k,2} \in \mathbb{C}^{N_s \times N_p}$, and $\mathbf{n}_k \sim \mathcal{CN}(0, \sigma_k^2 \mathbf{I})$ is additive Gaussian noise. The UCT transmit covariance per UCR is now $\mathbf{Q}_{k,s} = \mathbf{W}_k \mathbf{W}_k^H$, and the overall UCT transmit covariance assuming independent messages is $\mathbf{Q}_s = \sum_{k=1}^K \mathbf{Q}_{k,s}$.

We assume each UCR has a desired information rate of R_k , and adopt the ‘‘BD for power control’’ approach in [27, Sec. II-B]. Letting $\mathbf{W}_k = \mathbf{T}_k \Lambda_k^{1/2}$, it is possible to separately design the beamforming matrix \mathbf{T}_k and diagonal power allocation matrix Λ_k per user to achieve rate R_k in a two-step process.

Let

$$\mathbf{G}_{-k} = [\mathbf{G}_{1,1} \quad \cdots \quad \mathbf{G}_{k-1,1} \quad \mathbf{G}_{k+1,1} \quad \cdots \quad \mathbf{G}_{K,1}]$$

represent the the overall UCR downlink channel excluding the k^{th} user. First, a closed-form solution for the unit-power beamforming matrix \mathbf{T}_k of user k is obtained from the nullspace of \mathbf{G}_{-k} . To achieve this, from the SVD $\mathbf{G}_{-k} = \mathbf{U}_{-k} \mathbf{\Sigma}_{-k} [\mathbf{V}_{-k,1} \quad \mathbf{V}_{-k,0}]^H$, the last $(N_a - l_k)$ right singular vectors contained in $\mathbf{V}_{-k,0}$ can be used to construct \mathbf{T}_k [27]. The BD strategy therefore completely eliminates intra-UCR interference on the underlay downlink, and the residual interference-plus-noise covariance matrix at UCR k is

$$\mathbf{Z}_k = \mathbf{G}_{k,2} \mathbf{Q}_p \mathbf{G}_{k,2}^H + \sigma_s^2 \mathbf{I}. \quad (18)$$

Proceeding to the power allocation step, let $\text{rank}(\mathbf{G}_{k,1} \mathbf{T}_k) = r_k$ for user k 's effective channel, and assume $l_k = r_k$. Consider the SVD of user k 's pre-whitened effective channel

$$\mathbf{Z}_k^{-1/2} \mathbf{G}_{k,1} \mathbf{T}_k = \mathbf{U}_k \mathbf{\Lambda}_k \mathbf{V}_k^H$$

where $\mathbf{\Lambda}_k = \text{diag}(\lambda_{k,1}, \dots, \lambda_{k,r_k})$ is the power allocation matrix. While [27] computes $\mathbf{\Lambda}_k$ using the classic waterfilling algorithm in order to minimize the power required to achieve rate R_k , we can instead apply any of the other schemes discussed in Sec. III such as FWF. Due to the subadditivity of the rank function, reducing the rank of the per-user transmit covariances via FWF effectively reduces the rank of the overall UCT transmit covariance \mathbf{Q}_s , which in turn mitigates the interference caused to the PR according to Proposition 1.

VI. PRIMARY OUTAGE PROBABILITY

In this section we characterize the impact of the classic and frugal waterfilling methods on the primary receiver performance assuming independent Rayleigh fading on all channels. Herein, the channels are mutually independent and are each composed of i.i.d. zero-mean circularly symmetric complex Gaussian entries, i.e., $\text{vec}(\mathbf{G}_1) \sim \mathcal{CN}(\mathbf{0}, \mathbf{I})$, and the same distribution holds for $\mathbf{H}_1, \mathbf{H}_2$, and \mathbf{G}_2 .

A first approach would be to directly analyze the PR rate outage probability $I_r = \Pr(R_p(\mathbf{Q}_s) \leq T)$ for a target rate T , which is equivalent to

$$I_r = \Pr \left(\log_2 \left| \mathbf{I} + \mathbf{H}_1 \mathbf{Q}_p \mathbf{H}_1^H (\mathbf{K}_p + \sigma_p^2 \mathbf{I})^{-1} \right| \leq T \right) \quad (19)$$

where \mathbf{Q}_s and \mathbf{Q}_p are obtained via one of the waterfilling methods on their noise-prewhitened channels and are therefore functions of random matrices $\{\mathbf{G}_1, \mathbf{G}_2\}$ and $\{\mathbf{H}_1, \mathbf{H}_2\}$, respectively. Unfortunately, the computation of (19) is prohibitively complex since it is a non-linear function of the eigenvalues of four complex Gaussian random matrices (even if the PT applies uniform power allocation instead), and is an open problem to our best knowledge. Previous studies on the statistical distribution of MIMO capacity under interference usually circumvent this difficulty by assuming the MIMO transmitter and interferer adopt uniform or deterministic power allocation [28], [29], [37], which reduces the problem to one involving two complex Gaussian random matrices. As such, we are not aware of prior work on the statistics of

MIMO capacity under interference where either one or both transmitters employ waterfilling as in our model.

In light of the above, it is of interest to develop more tractable PR performance measures. One such candidate is the PR interference temperature outage probability (ITOP), which is the probability that $T_p(\mathbf{Q}_s)$ [cf. (4)] exceeds a threshold η :

$$I_p(\mathbf{Q}_s, \eta) = \Pr(\text{Tr}(\mathbf{H}_2 \mathbf{Q}_s \mathbf{H}_2^H) \geq \eta). \quad (20)$$

The ITOP is appealing since the interference temperature metric is widely used in underlay systems, and can be considered to be the MIMO counterpart of efforts to characterize the statistical distribution of aggregate UCT interference in single-antenna networks as in [30]. Paradoxically, however, it is seen in Sec. VII that FWF causes the highest ITOP, even though the average primary rate is the highest and the PR rate outage is the lowest when \mathbf{Q}_s is computed using FWF. Therefore, a more accurate surrogate for the PR rate outage I_r is the interference leakage-rate outage probability (ILOP), defined as

$$I_l(\mathbf{Q}_s, \eta) = \Pr(\log_2 |\sigma_p^2 \mathbf{I} + \mathbf{H}_2 \mathbf{Q}_s \mathbf{H}_2^H| \geq \eta), \quad (21)$$

and it is verified in Sec. VII that UCT transmission schemes with the lowest ILOP also minimize I_r . This is because the leakage rate has a direct impact on the PR rate: $R_p(\mathbf{Q}_s)$ in (5) can be rewritten as

$$R_p(\mathbf{Q}_s) = \log_2 |\sigma_p^2 \mathbf{I} + \mathbf{H}_1 \mathbf{Q}_p \mathbf{H}_1^H + \mathbf{K}_p| - \log_2 |\sigma_p^2 \mathbf{I} + \mathbf{K}_p| \quad (22)$$

where the first term is the sum rate of the virtual PT/UCT multiple access channel (MAC) with optimal successive detection, and the second term is the leakage rate from the UCT. For the worst-case scenario where the PT is decoded first in the virtual MAC, decreasing the leakage rate improves the detection of the PT signal in the first term and simultaneously reduces the second term, thereby decreasing I_r . On the other hand, the link between interference temperature and PR rate is more tenuous.

Assume the UCT transmit covariance matrix \mathbf{Q}_s is of rank k , $1 \leq k \leq \min(N_a, N_s)$, where k is determined by the choice of waterfilling scheme to achieve rate R_b over the pre-whitened UCT channel $\tilde{\mathbf{G}}_1 \triangleq (\mathbf{K}_s + \sigma_s^2 \mathbf{I})^{-1/2} \mathbf{G}_1$. Assume $\tilde{\mathbf{G}}_1^H \tilde{\mathbf{G}}_1$ is of rank d' , with non-zero ordered eigenvalues $\{\alpha_i\}_{i=1}^{d'}$. Waterfilling yields a diagonal \mathbf{Q}_s with entries [16]

$$[\mathbf{Q}_s]_{i,i} = \left[\mu - \frac{\sigma_s^2}{\alpha_i} \right]^+, \quad i = 1, \dots, N_a, \quad (23)$$

where the waterfilling level μ is a function of P_s , σ_s^2 , and $\boldsymbol{\alpha} = (\alpha_1, \dots, \alpha_{d'})$ [31], [33]. Similar arguments hold for the underlay downlink covariance \mathbf{Q}_s designed for sum-rate target $\sum_k R_k$ and aggregate channel $\tilde{\mathbf{G}} = \left[\left(\mathbf{Z}_1^{-1/2} \mathbf{G}_{1,1} \mathbf{T}_1 \right)^T \quad \cdots \quad \left(\mathbf{Z}_K^{-1/2} \mathbf{G}_{K,1} \mathbf{T}_K \right)^T \right]$.

A. Interference Temperature Outage Probability

Noting that the ITOP and ILOP (20)-(21) are still functions of four complex Gaussian matrices, we first develop bounds

on the ITOP as follows. We assume \mathbf{H}_2 is full rank such that $\text{rank}(\mathbf{H}_2) = d = \min(N_r, N_a)$, which holds with probability 1 under i.i.d. Rayleigh fading. Define $r = \min(k, d)$ and let $\lambda_i(\mathbf{A})$ denote the i^{th} ordered eigenvalue of \mathbf{A} in descending order. Starting with the commutativity of the trace operator,

$$I_p = \Pr(\text{Tr}(\mathbf{H}_2^H \mathbf{H}_2 \mathbf{Q}_s) \geq \eta) \quad (24)$$

$$\leq \Pr(\text{Tr}(\mathbf{H}_2^H \mathbf{H}_2 \mathbf{Q}_s | \mathbf{Q}_p = (P_p/N_p)\mathbf{I}) \geq \eta) \quad (25)$$

$$= \Pr\left(\sum_{i=1}^r \lambda_i(\mathbf{H}_2^H \mathbf{H}_2 \mathbf{Q}_s) \geq \eta\right) \quad (26)$$

$$\approx \Pr\left(\sum_{i=1}^r \lambda_i(\mathbf{H}_2^H \mathbf{H}_2 \tilde{\mathbf{Q}}_s) \geq \eta\right) \quad (27)$$

$$\leq \Pr\left(\sum_{i=1}^r \lambda_i(\mathbf{H}_2^H \mathbf{H}_2) \lambda_i(\tilde{\mathbf{Q}}_s) \geq \eta\right) \quad (28)$$

$$\leq \Pr\left(\lambda_1(\tilde{\mathbf{Q}}_s) \sum_{i=1}^r \lambda_i(\mathbf{H}_2^H \mathbf{H}_2) \geq \eta\right) \quad (29)$$

where in (25) we eliminate dependence on \mathbf{H}_1 by assuming the PT adopts uniform power allocation ($\mathbf{Q}_p = (P_p/N_p)\mathbf{I}$) such that $\mathbf{K}_s = (P_p/N_p)\mathbf{G}_2\mathbf{G}_2^H$, which is a worst-case interference scenario at the UCR according to Proposition 1 and potentially increases the power expended by the UCT; in (27) $\tilde{\mathbf{Q}}_s$ is the statistical waterfilling solution where μ in (23) is a function of the statistics of $\{\alpha_i\}_{i=1}^d$ and offers nearly the same performance as instantaneous waterfilling [31]-[33]; and the inequality in (28) follows from the bound on the trace of a product of Hermitian matrices [34].

We now define the ordered eigenvalue vectors $\mathbf{h} = (\lambda_1(\mathbf{H}_2^H \mathbf{H}_2), \dots, \lambda_r(\mathbf{H}_2^H \mathbf{H}_2))$ and $\mathbf{q} = (\lambda_1(\tilde{\mathbf{Q}}_s), \dots, \lambda_r(\tilde{\mathbf{Q}}_s))$. Observe that the overall joint density of these random eigenvalues is given by the product of the individual joint densities: $f_{\mathbf{h}, \mathbf{q}}(\mathbf{h}, \mathbf{q}) = f_{\mathbf{h}}(\mathbf{h}) f_{\mathbf{q}}(\mathbf{q})$ due to the independence of the associated channel matrices. Thus, the bound in (29) can be rewritten as

$$I_p \leq E_{\mathbf{h}} \left\{ 1 - F_{q_1} \left(\eta / \sum_{i=1}^r h_i \right) \right\} \quad (30)$$

where $F_{q_1}(x)$ is the cumulative distribution function (cdf) of the largest eigenvalue q_1 . From (23) we obtain $F_{q_1}(x) = F_{\alpha_1}(\sigma_s^2/(\bar{\mu} - x))$ where $\bar{\mu}$ is the statistical water level. The cdf of α_1 , the largest eigenvalue of $\tilde{\mathbf{G}}_1^H \tilde{\mathbf{G}}_1$, is given next for the scenario $N_s \geq N_a, N_s \geq N_p$.

Lemma 1: [38] Given complex Gaussian matrices $\mathbf{X} \in \mathbb{C}^{N_s \times N_a}, \mathbf{Y} \in \mathbb{C}^{N_s \times N_p}$, and $(N_p \times N_p)$ diagonal matrix $\mathbf{P} = \text{diag}(\rho, \dots, \rho)$, the cdf of the largest eigenvalue α_{max} of the quadratic form $\mathbf{X}^H (\mathbf{Y} \mathbf{P} \mathbf{Y}^H + \sigma^2 \mathbf{I}) \mathbf{X}$ when $N_s \geq N_a, N_s \geq N_p$ is

$$F_{\alpha_{max}}(x) = K_1 \left| \tilde{\Delta}_1(x) \right| \quad (31)$$

$$\text{where } \tilde{\Delta}_1(x) = \begin{bmatrix} \tilde{\mathbf{Y}}(x)^T & \mathbf{Z}^T \end{bmatrix}^T,$$

$$\left[\tilde{\mathbf{Y}}(x) \right]_{i,j} = \begin{cases} \Gamma(i) I_{N_a-i}(\rho) - \Gamma(i) e^{-x} \\ \times \sum_{k=0}^{i-1} \frac{x^k}{k!} I_{N_a-i} \left(\frac{\rho}{1+\rho x} \right), & i = 1, \dots, N_a, \\ (-1)^{N_s-j} I_{N_a+N_s-i}(\rho), & i = N_a + 1, \dots, N_s, \end{cases}$$

$I_a(b) = \sum_{k=0}^a \binom{a}{k} b^{j+k} \Gamma(j+k)$, and the normalization constant K_1 [38, eq. (25)] and the entries $[\mathbf{Z}]_{i,j}$ [38, eq. (27)] are functions of the array dimensions independent of x .

The cdf $F_{\alpha_1}(x)$ for other antenna array dimensions is of a similar form and can be found in [38]. Now, in order to compute the expectation over \mathbf{h} in (30), we exploit the Gaussian distribution of \mathbf{H}_2 based on the following lemma.

Lemma 2: [16], [35] If \mathbf{X} is a $(N_r \times N_a)$ matrix with i.i.d. zero-mean unit-variance complex Gaussian elements, then $\mathbf{W} = \mathbf{X}\mathbf{X}^H$ follows a central complex Wishart distribution if $N_r \leq N_a$, otherwise $\mathbf{W} = \mathbf{X}^H \mathbf{X}$ is Wishart-distributed if $N_r > N_a$. Given $c \triangleq \max(N_r, N_a)$ and $m \triangleq \min(N_r, N_a)$, the joint density of all m ordered eigenvalues of \mathbf{W} is

$$f_{\Lambda}(\lambda_1, \dots, \lambda_m) = K_w |\mathbf{V}_1(\boldsymbol{\lambda})|^2 \prod_{i=1}^m \frac{e^{-\lambda_i}}{(\lambda_i)^{m-c}}, \quad (32)$$

where $\mathbf{V}_1(\boldsymbol{\lambda})$ is a Vandermonde matrix with entries $[\mathbf{V}_1(\boldsymbol{\lambda})]_{i,j} = \lambda_j^{i-1}$, and K_w is a normalization constant independent of $\boldsymbol{\lambda}$ [35, eq. 7].

For the case where $\text{rank}(\tilde{\mathbf{Q}}_s) = k$ is greater than $\text{rank}(\mathbf{H}_2) = d$, i.e., $r = d$, the term $\sum_{i=1}^r h_i$ in (30) involves all d ordered eigenvalues $\{h_1, \dots, h_d\}$ and the associated joint density function $f_{\mathbf{h}}(\mathbf{h})$ is given in Lemma 2. Thus (30) yields

$$I_p \leq 1 - K \int \dots \int_{\mathfrak{D}} \left| \tilde{\Delta}_1(\bar{h}) \right| |\mathbf{V}_1(\mathbf{h})| \prod_{i=1}^d \xi(h_i) d\mathbf{h} \quad (33)$$

where $K = K_1 K_w$, $\bar{h} = \sigma_s^2 / (\bar{\mu} - \eta / \sum_{i=1}^d h_i)$, $\xi(h_i) = \frac{e^{-h_i}}{(h_i)^{m-c}}$, and the integration region is $\mathfrak{D} = \{\infty \geq h_1 \geq h_2 \geq \dots \geq h_d \geq 0\}$. This multidimensional integral has a closed-form solution obtained from the following generalized Cauchy-Binet identity.

Lemma 3: [40, Lemma 2] For $\mathbf{x} = \{x_1, \dots, x_M\}$, arbitrary integrable functions $c_i(\cdot)$, $u_i(\cdot)$, and $\varphi(\cdot)$, $N \times N$ matrix $\Phi(\mathbf{x})$ and $M \times M$ matrix $\Psi(\mathbf{x})$ ($M \leq N$), where $\Phi(\mathbf{x}) = \begin{bmatrix} \mathbf{C}_1(\mathbf{x})^T & \mathbf{C}_2^T \end{bmatrix}^T$, with entries $[\mathbf{C}_1(\mathbf{x})]_{i,j} = c_i(x_j)$ for $i = 1, \dots, N - M; j = 1, \dots, N$, $[\mathbf{C}_2]_{i,j} = c_{2i,j}$ (constant scalars) for $i = N - M + 1, \dots, N; j = 1, \dots, N$, and $[\Psi(\mathbf{x})]_{i,j} = u_i(x_j)$, the following integral identity over domain $\mathfrak{D} = \{b \geq x_1 \geq x_2 \geq \dots \geq x_N \geq a\}$ holds:

$$\int \dots \int_{\mathfrak{D}} |\Phi(\mathbf{x})| \cdot |\Psi(\mathbf{x})| \prod_{k=1}^N \varphi(x_k) dx = M! \det \mathbf{B} \quad (34)$$

where

$$[\mathbf{B}]_{i,j} = \begin{cases} \int_a^b \varphi(x) c_j(x) u_i(x) dx, & i = 1, \dots, N - M; \forall j \\ c_{2i,j}, & i = N - M + 1, \dots, N; \forall j. \end{cases} \quad (35)$$

A compact solution to (33) is then obtained by setting $\Phi = \tilde{\Delta}_1(\bar{h})$ with $\rho = P_p/N_p$, $\Psi(\mathbf{x}) = \mathbf{V}_1(\mathbf{h})$, and $\varphi(x) = \xi(h)$ in Lemma 3:

$$I_p \leq 1 - d! K |\mathbf{B}_1|; \quad (36)$$

$$[\mathbf{B}_1]_{i,j} = \begin{cases} \int_0^\infty \xi(x) x_j^{i-1} \left[\tilde{\mathbf{Y}}(x) \right]_{i,j} dx, & i = 1, \dots, N - M; \forall j \\ [\mathbf{Z}]_{i,j}, & i = N - M + 1, \dots, N; \forall j. \end{cases} \quad (37)$$

and requires a computationally-inexpensive one-dimensional numerical integration of the product of elementary functions in (37).

On the other hand, when $r = k < d$, only the k largest eigenvalues are included in the term $\sum_{i=1}^r h_i$ in (30), which necessitates invoking the corresponding joint density function given below in Lemma 4.

Lemma 4: [39] The joint density function of the ordered subset of the s largest eigenvalues of Wishart matrix \mathbf{W} having m non-zero eigenvalues in total is

$$f_{\lambda_1, \dots, \lambda_s}(\lambda) = K_w \sum_{\mathbf{n}, \mathbf{m}, s} \sum_{\mathbf{m}, \mathbf{s}} \text{sgn}(\mathbf{n}, \mathbf{m}) |\mathbf{D}(\lambda_s)| \times \prod_l^s e^{-1} \lambda_l^{N_r - N_a + n_l - m_l + 2} \quad (38)$$

where $\mathbf{n} = \mathbf{m} = \{1, \dots, s\}$, each summation is a N_r -fold nested sum over permutations $r_{i,\mathbf{n}}, r_{j,\mathbf{m}}$ of the index sets as defined in [39, eq. (16)] with sign determined by $\text{sgn}(\mathbf{n}, \mathbf{m}) \in \{\pm 1\}$ [39, eq. (17)],

$$[\mathbf{D}(\lambda_s)]_{i,j} = \gamma(N_a - N_r + r_{i,\mathbf{n}} + r_{j,\mathbf{m}}, \lambda_s), \quad (39)$$

and $\gamma(a, b)$ is the incomplete gamma function [38].

Substituting $\varphi(x_k) = x_k^{N_r - N_a + n_l - m_l + 2}$ and associated expressions into (30) and invoking Lemma 3 provides

$$I_p \leq 1 - \frac{k!K}{e^k} \sum_{\mathbf{n}, \mathbf{d}, k} \sum_{\mathbf{m}, \mathbf{d}, k} \text{sgn}(\mathbf{n}, \mathbf{m}) |\mathbf{B}_2| \quad (40)$$

where

$$[\mathbf{B}_2]_{i,j} = \begin{cases} \int_0^\infty \varphi(x_k) [\mathbf{D}(x)]_{i,j} [\tilde{\mathbf{Y}}(x)]_{i,j} dx, & i = 1, \dots, d - k \\ [\mathbf{Z}]_{i,j}, & i = d - k + 1, \dots, N; \forall j. \end{cases} \quad (41)$$

Since $\gamma(a, b)$ is a standard function in MATLAB, the numerical integration of its product with two elementary functions in (41) is straightforward.

B. Interference Leakage Outage Probability

Turning our attention to the ILOP, starting with the definition of I_l we have

$$I_l(\mathbf{Q}_s, \eta) = \Pr\left(\sum_{i=1}^r \log_2(\sigma_p^2 + \lambda_i(\mathbf{Q}_s \mathbf{H}_2^H \mathbf{H}_2)) \geq \eta\right) \approx \Pr\left(\log_2 \prod_{i=1}^r \lambda_i(\mathbf{Q}_s \mathbf{H}_2^H \mathbf{H}_2) \geq \eta\right) \quad (42)$$

$$\leq \Pr\left(\prod_{i=1}^r \lambda_i(\tilde{\mathbf{Q}}_s) \lambda_i(\mathbf{H}_2 \mathbf{H}_2^H) \geq 2^\eta\right) \quad (43)$$

$$\leq \Pr\left((q_1)^r \prod_{i=1}^r h_i \geq 2^\eta\right) \quad (44)$$

$$= E_h \left\{ 1 - F_{q_1} \left(2^\eta / \prod_{i=1}^r h_i \right)^{1/r} \right\} \quad (45)$$

where in (42) we consider the interference-limited scenario which is of interest, and (43) is due to [34].

The computation of (45) closely parallels that of (30), by again separating the cases $r = d < k$ and $r = k < d$, followed by invoking Lemmas 1–3 for the former and Lemmas 1, 4 and 3 for the latter case, respectively. Therefore, the resulting closed-form bounds for the ILOP are of the form in (36) and (40), with $\bar{h} = (2^\eta / \prod_{i=1}^r h_i)^{1/r}$ and all other terms being unchanged.

VII. NUMERICAL RESULTS

In this section, we present some numerical examples to demonstrate the performance of the proposed rank-minimization UCT transmit covariance designs in MIMO cognitive radio networks. We consider MIMO cognitive radio networks with one primary user and one or more underlay receivers. In all simulations, the channel matrices and background noise samples were assumed to be composed of independent, zero-mean Gaussian random variables with unit variance. In situations where the desired rate for UCT cannot be achieved with the given P_s , rather than indicate an outage, we simply assign all power to transmit signals. The performance is evaluated by averaging over 1000 independent channel realizations.

A. Single Underlay Receiver Scenario

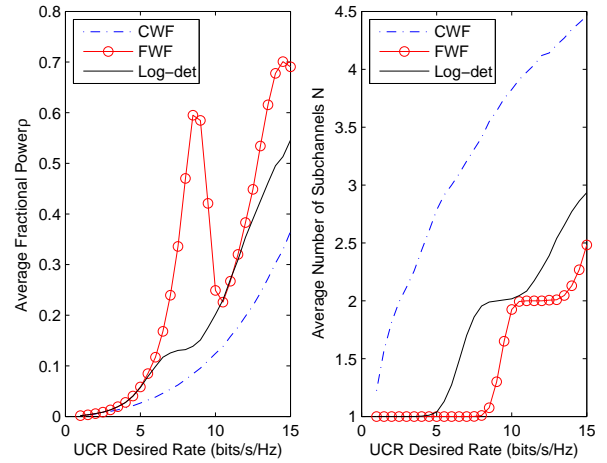


Fig. 2. Power and dimension allocation versus UCR desired rate.

We first consider the single UCR scenario, where each node is equipped with 6 antennas, and $P_s = 100$, $P_p = 10$. Fig. 2 illustrates the average fractional power ρ and the average number of subchannels N required to achieve the UCR desired rates by CWF, FWF and log-det heuristic algorithms. It is shown that the trace and rank of the UCT transmit covariance matrix \mathbf{Q}_s are two competing objectives, and any scheme which requires more power occupies fewer spatial dimensions. Among the three methods, CWF demands the largest spatial footprint, while the FWF scheme offers the smallest feasible number of transmit dimension. We should point out that the log-det heuristic algorithm for matrix rank minimization does not always provide the smallest transmit dimension, compared to FWF. This is because the log-det algorithm is an approximate heuristic and can only give a local minimum.

The achieved average primary user data rates for all the methods is depicted in Fig. 3. As expected, the lower-rank UCT transmit covariance will cause lesser degradation on average to the PU communication link, thus resulting a higher PR rate in accordance with Proposition 1. Compared to CWF, either of the proposed modified waterfilling algorithms or the

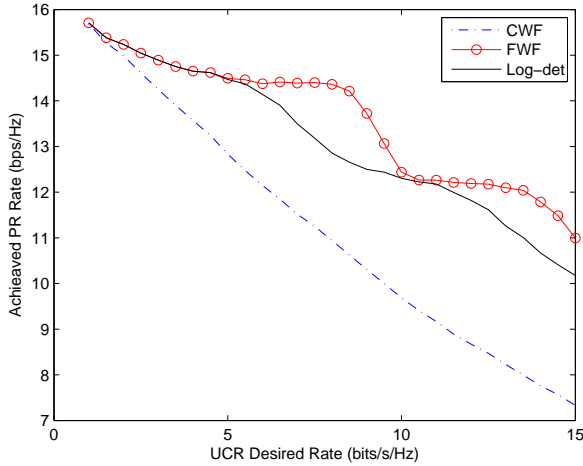


Fig. 3. Achieved PU rate versus UCR desired rate.

log-det heuristic lead to more desirable PR rates, with the advantage of FWF being more pronounced as R_b increases.

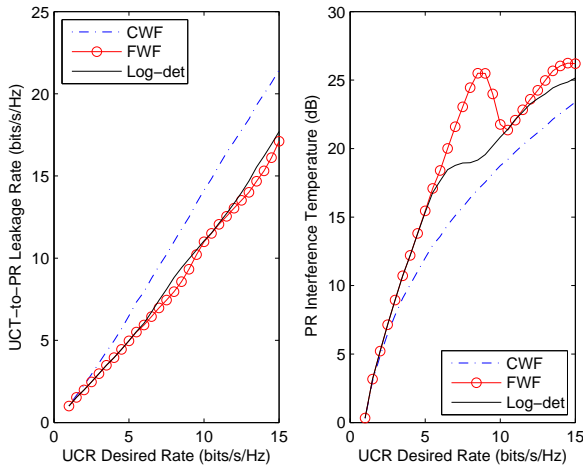


Fig. 4. Two metrics of PR Interference versus UCR desired rate.

To obtain greater insight, Fig. 4 compares two metrics of interference at PR using different algorithms, where one is the newly-defined UCT-PR leakage rate, the other one is the commonly-used interference temperature. We notice that an interesting phenomenon: the two metrics gives the opposite trend. It is worth to point out that the commonly-used interference temperature metric does not accurately capture the interference impact caused by the UCT on the primary mutual information, while the interference leakage rate remedies this defect.

For the statistical characterization of the proposed schemes, we exhibit the empirical complementary cdfs and select analytical upper bounds from Sec. VI of the interference temperature and leakage rate metrics in Fig. 5, for 6 antennas at all users and $P_s = 200$, $R_b = 8$, $P_p = 40$. An immediate observation is the conflicting trends of the leakage and temperature metrics: FWF causes a much greater interference temperature outage

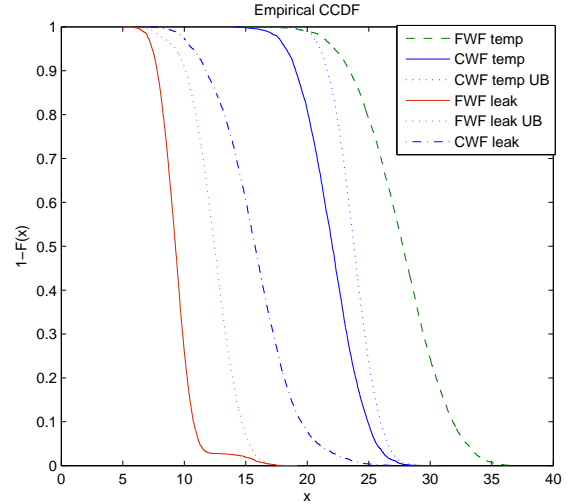


Fig. 5. Empirical cdf of interference temperature and leakage rate under CWF and FWF.

and much smaller leakage rate outage compared to CWF, and the superiority of one versus the other is not apparent. To resolve this dilemma, the corresponding empirical PR rate cdfs are shown in Fig. 6, and it is clear that employing FWF leads to a very significant reduction in PR rate outage probability as compared to CWF. Furthermore, the interference temperature outage is again seen to be misleading regarding the true impact on the PR rate outage probability. Thus, FWF outperforms CWF in terms of both average PR rate and PR rate outage probability.

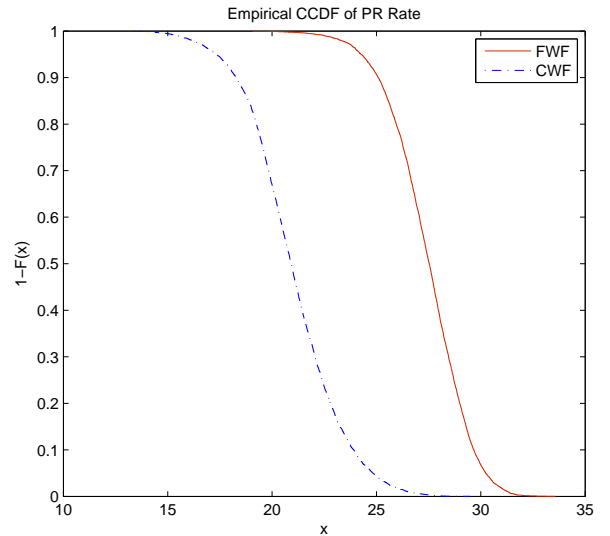


Fig. 6. Empirical cdf of PR rate under CWF and FWF.

B. MIMO Underlay Downlink Scenario

Next, we evaluate the performance of the proposed algorithms with the modified BD strategy of Sec. V for a MIMO underlay downlink system, where there are $K = 3$ UCRs, and

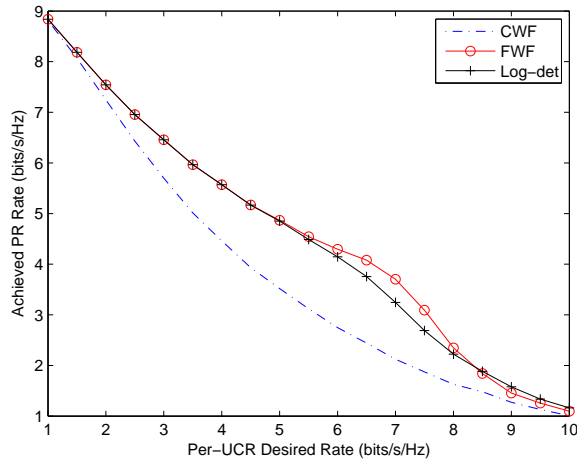


Fig. 7. Achieved PR rate versus per-UCR desired rate in MIMO underlay downlink, $P_s = 20dB$, $P_p = 10dB$.

$N_a = 12$, $N_p = N_r = N_s = 4$. Without loss of generality it is assumed that the desired rate targets for all UCRs are the same, i.e. $R_1 = R_2 = R_3$. Fig. 7 illustrates the achieved PU rate versus per UCT desired rate, when $P_s = 100$ or $20dB$ and $P_p = 10$ or $10dB$. The benefit of minimizing the transmit covariance rank is seen to hold even for the multi-user downlink scenario.

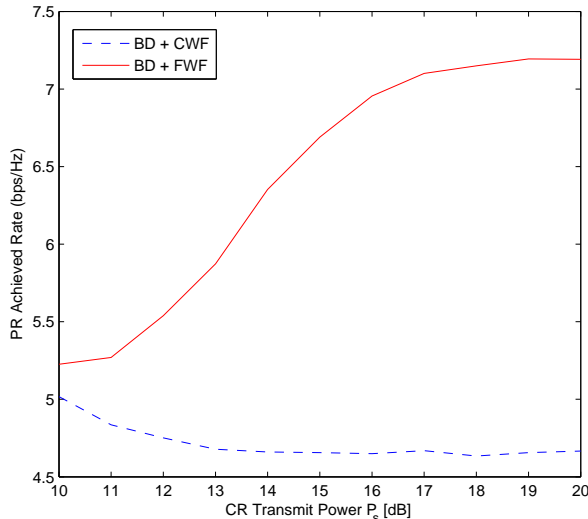


Fig. 8. Achieved PR rate versus UCT transmit power in MIMO downlink system with identical target rates $R_1 = R_2 = R_3 = 5$ bits/s/Hz.

It is also of interest to see how the achieved PR rates under the various designs vary with the UCT transmit power, when the desired rate for each UCT is fixed. The simulation settings are the same as above, except that we fix $R_1 = R_2 = R_3 = 5$ and $P_s \in [10dB, 20dB]$. The results are shown in Fig. 8, with the corresponding leakage rate and interference temperature metrics in Fig. 9. Once again, FWF offers the optimal average PR rate and PR rate outage probability in the downlink scenario.

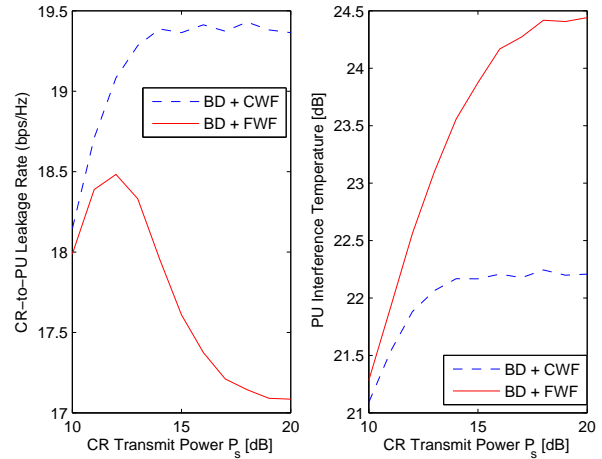


Fig. 9. Two metrics of PR interference versus UCT transmit power in MIMO underlay downlink with identical target rates $R_1 = R_2 = R_3 = 5$.

VIII. CONCLUSION

This paper has proposed a rank minimization precoding strategy for underlay MIMO CR systems with completely unknown primary CSI, assuming a minimum information rate must be guaranteed on the CR main channel. We presented a simple waterfilling approach can be used to find the minimum rank transmit covariance that achieves the desired CR rate with minimum power. We also presented two alternatives to FWF that are based on convex approximations to the minrank criterion, one that leads to conventional waterfilling for our CR problem, and another based on a log-det heuristic. The CWF approach turns out to be a poor approximation to the min-rank objective, while the log-det approach provides performance similar to FWF, although FWF consistently leads to the highest throughput for the primary link. We also observed that reducing the interference temperature metric is surprisingly not consistent with improving the PR throughput; in particular, FWF has the highest interference temperature of the algorithms studied, but also leads to the highest PR rate. As an alternative, we proposed an interference leakage metric that is a better indicator of the impact of the CR on the primary link.

REFERENCES

- [1] A. Goldsmith, S. A. Jafar, I. Maric, and S. Srinivasa, "Breaking spectrum gridlock with cognitive radios: An information theoretic perspective," *Proc. IEEE*, vol. 97, no. 5, pp. 894-914, May 2009.
- [2] L. B. Le and E. Hossain, "Resource allocation for spectrum underlay in cognitive wireless networks," *IEEE Trans. Wireless Commun.*, vol. 7, no. 12, pp. 5306-5315, Dec. 2008.
- [3] R. Zhang and Y. C. Liang, "Exploiting multi-antennas for opportunistic spectrum sharing in cognitive radio networks," *IEEE J. Sel. Topics Signal Proc.*, vol. 2, no. 1, pp. 88-102, Feb. 2008.
- [4] K. Hamdi, W. Zhang and K. B. Letaief, "Opportunistic spectrum sharing in cognitive MIMO wireless networks," *IEEE Trans. Wireless Commun.*, vol. 8, no. 8, pp. 4098-4111, Aug. 2009.
- [5] A. Tajer, N. Prasad, and X. Wang, "Beamforming and rate allocation in MISO cognitive radio networks," *IEEE Trans. Signal Proc.*, vol. 58, no. 1, pp. 362-377, Jan. 2010.
- [6] L. Zhang, Y.-C. Liang, Y. Xin, and H. V. Poor, "Robust cognitive beamforming with partial channel state information," *IEEE Trans. Wireless Commun.*, vol. 8, no. 8, pp. 4143-4153, Aug. 2009.

- [7] E. A. Gharavol, Y.-C. Liang, and K. Mouthaan, "Robust linear transceiver design in MIMO ad hoc cognitive radio networks with imperfect channel state information," *IEEE Trans. Wireless Commun.*, vol. 10, no. 5, pp. 1448-1457, May 2011.
- [8] E. A. Gharavol, Y.-C. Liang, and K. Mouthaan, "Robust downlink beamforming in multiuser MISO cognitive radio networks with imperfect channel-state information," *IEEE Trans. Veh. Tech.*, vol. 59, no. 6, pp. 2852-2867, Jul. 2010.
- [9] K. T. Phan, S. A. Vorobyov, N. D. Sidiropoulos, and C. Tellambura, "Spectrum sharing in wireless networks via QoS-aware secondary multicast beamforming," *IEEE Trans. Signal Proc.*, vol. 57, no. 6, pp. 2323-2335, Jun. 2009.
- [10] H. Yi, H. Hu, Y. Rui, K. Guo, and J. Zhang, "Null space-based precoding scheme for secondary transmission in a cognitive radio MIMO system using second-order statistics," *Proc. of IEEE ICC*, 2009.
- [11] Z. Chen, C.-X. Wang, X. Hong, J. S. Thompson, S. A. Vorobyov, F. Zhao, H. Xiao, and X. Ge, "Interference mitigation for cognitive radio MIMO systems based on practical precoding," [Online]. Available: <http://arxiv.org/abs/1104.4155>.
- [12] Y. Zhang and A. So, "Optimal spectrum sharing in MIMO cognitive radio networks via semidefinite programming," *IEEE J. Sel. Areas Commun.*, vol. 29, no. 2, pp. 362-373, Feb. 2011.
- [13] Y. Noam and A. Goldsmith, "Blind null-space learning for MIMO underlay cognitive radio networks," [Online]. Available: <http://arxiv.org/abs/1202.0366>.
- [14] D. S. Papailiopoulos and A. G. Dimakis, "Interference alignment as a rank constrained rank minimization," *Proc. of IEEE GLOBECOM*, 2010.
- [15] S. A. Jafar, "Blind interference alignment," to appear, *IEEE J. Sel. Topics Signal Proc.*, 2012. Available on *Early Access*.
- [16] I. E. Telatar, "Capacity of multi-antenna Gaussian channels," *Eur. Trans. Telecomm.*, vol. 10, no. 6, pp. 585C-595, Nov. 1999.
- [17] J. G. Andrews, W. Choi and R. W. Heath, "Overcoming interference in spatial multiplexing MIMO wireless networks," *IEEE Wireless Commun. Mag.*, vol. 14, no. 6, pp. 95-104, Dec. 2007.
- [18] G. Arslan, M. F. Demirkol, and Y. Song, "Equilibrium efficiency improvement in MIMO interference systems: A decentralized stream control approach," *IEEE Trans. Wireless Commun.*, vol. 6, no. 8, pp. 2984-2993, June 2007.
- [19] A. Mukherjee and A. L. Swindlehurst, "Modified waterfilling algorithms for MIMO spatial multiplexing with asymmetric CSI," to appear, *IEEE Wireless Comm. Lett.*, 2012. Available on *Early Access*.
- [20] A. Mukherjee and A. L. Swindlehurst, "Fixed-rate power allocation strategies for enhanced secrecy in MIMO wiretap channels," *Proc. of IEEE SPAWC*, pp. 344-348, 2009.
- [21] R. S. Blum, "MIMO capacity with interference," *IEEE J. Sel. Areas Commun.*, vol. 21, no. 5, pp. 793-801, June 2003.
- [22] M. Fazel, H. Hindi and S. P. Boyd, "A rank minimization heuristic with application to minimum order system approximation," *Proc. Amer. Control Conf.*, vol. 6, pp. 4734-4739, Jun. 2001.
- [23] M. Fazel, H. Hindi and S. P. Boyd, "Log-det heuristic for matrix rank minimization with applications to Hankel and Euclidean distance matrices," *Proc. Amer. Control Conf.*, pp. 2156-2162, Jun. 2003.
- [24] H. Yu and V. K. N. Lau, "Rank-constrained Schur-convex optimization with multiple trace/log-det constraints," *IEEE Trans. Signal Proc.*, vol. 59, no. 1, pp. 304-314, Jan. 2011.
- [25] A. Kashyap, T. Basar and R. Srikant, "Correlated jamming on MIMO Gaussian fading channels" *IEEE Trans. Inf. Theory*, vol. 50, no. 9, pp. 2119-2223, Sept. 2004.
- [26] W. Mao, X. Su, and X. Xu, "Comments on 'Correlated Jamming on MIMO Gaussian Fading Channels'," *IEEE Trans. Inf. Theory*, vol. 52, no. 11, pp. 5163-5165, Nov. 2006.
- [27] Q. Spencer, A. L. Swindlehurst, and M. Haardt, "Zero-forcing methods for downlink spatial multiplexing in multi-user MIMO channels," *IEEE Trans. Signal Proc.*, vol. 52, no. 2, pp. 461-471, Feb. 2004.
- [28] A. Lozano and A. M. Tulino, "Capacity of multiple-transmit multiple-receive antenna architectures," *IEEE Trans. Inf. Theory*, vol. 48, no. 12, pp. 3117-3128, Dec. 2002.
- [29] A. L. Moustakas, S. H. Simon, and A. M. Sengupta, "MIMO capacity through correlated channels in the presence of correlated interferers and noise: A (not so) large N analysis," *IEEE Trans. Inf. Theory*, vol. 49, no. 10 pp. 2545-2561, Oct. 2003.
- [30] T. Clancy, "Achievable capacity under the interference temperature model," *Proc. of IEEE INFOCOM*, May 2007.
- [31] Y.-C. Liang, R. Zhang, and J. M. Cioffi, "Subchannel grouping and statistical water-filling for vector block fading channels," *IEEE Trans. Commun.*, vol. 54, no. 6, pp. 1131-1142, June 2006.
- [32] J. H. Sung and J. R. Barry, "Approaching the zero-outage capacity of MIMO-OFDM without instantaneous water-filling," *IEEE Trans. Inf. Theory*, vol. 54, no. 4, pp. 1423-1436, Apr. 2008.
- [33] A. Zanella and M. Chiani, "Analytical comparison of power allocation methods in MIMO systems with singular value decomposition," *Proc. of IEEE GLOBECOM*, 2009.
- [34] F. Zhang and Q. Zhang, "Eigenvalue inequalities for matrix product," *IEEE Trans. Auto. Control*, vol. 51, no. 9, pp. 1506-1509, Sep. 2006.
- [35] M. Chiani, M. Z. Win, and A. Zanella, "On the capacity of spatially correlated MIMO channels," *IEEE Trans. Inf. Theory*, vol. 49, no. 10, pp. 2363-2371, Oct. 2003.
- [36] A. M. Tulino and S. Verdú, "Random matrix theory and wireless communications," *Found. Trends Commun. Inf. Theory*, vol. 1, no. 1, pp. 1163, 2004.
- [37] G. Alfano, A. Lozano, A. M. Tulino, and S. Verdú, "Eigenvalue statistics of finite-dimensional random matrices for MIMO wireless communications," *Proc. of IEEE ICC*, pp. 4125-4129, June 2006.
- [38] H. Kang, J. S. Kwak, T. G. Pratt, and G. L. Stüber, "Analytical framework for optimal combining with arbitrary-power co-channel interferers and thermal noise," *IEEE Trans. Veh. Tech.*, vol. 57, no. 3, pp. 1564-1575, May 2008.
- [39] A. Zanella, M. Chiani, and M. Z. Win, "On the marginal distribution of the eigenvalues of Wishart matrices," *IEEE Trans. Commun.*, vol. 57, no. 4, pp. 1050-1060, Apr. 2009.
- [40] H. Shin, M. Z. Win, J. Lee, and M. Chiani, "On the capacity of doubly correlated MIMO channels," *IEEE Trans. Wireless Commun.*, vol. 5, no. 8, pp. 2253-2265, Aug. 2006.